Reconfigurable Intelligent Surface Optimization for Uplink Sparse Code Multiple Access

Ibrahim Al-Nahhal, *Member, IEEE*, Octavia A. Dobre, *Fellow, IEEE*, Ertugrul Basar, *Senior Member, IEEE*, Telex M. N. Ngatched, *Senior Member, IEEE*, and Salama Ikki, *Senior Member, IEEE*

Abstract— The reconfigurable intelligent surface (RIS)-assisted sparse code multiple access (RIS-SCMA) is an attractive scheme for future wireless networks. In this letter, for the first time, the RIS phase shifts of the uplink RIS-SCMA system are optimized based on the alternate optimization (AO) technique to improve the received signal-to-noise ratio (SNR) for a discrete set of RIS phase shifts. The system model of the uplink RIS-SCMA is formulated to utilize the AO algorithm. For further reduction in the computational complexity, a low-complexity AO (LC-AO) algorithm is proposed. The complexity analysis of the two proposed algorithms is performed. Monte Carlo simulations and complexity analysis show that the proposed algorithms significantly improve the received SNR compared to the non-optimized RIS-SCMA scenario. The LC-AO provides the same received SNR as the AO algorithm, with a significant reduction in complexity. Moreover, the deployment of RISs for the uplink RIS-SCMA is investigated.

Index Terms— Sparse code multiple access (SCMA), reconfigurable intelligent surface (RIS), phase shift optimization, discrete phase shifts.

I. INTRODUCTION

RECONFIGURABLE intelligent surface (RIS)-empowered communication has recently become a promising candidate technology for future wireless networks. An RIS consists of low-cost passive elements that reflect the incident signals after adjusting their phases and/or amplitudes [1], [2]. By intelligent configuration of the incident signals' phases and/or amplitudes, the constructive and destructive interference between the reflected signals can be manipulated. Thus, the transmission environment of the wireless medium and quality-of-service can be improved without the need for coding [3].

Sparse code multiple access (SCMA) is a code-domain non-orthogonal multiple access (NOMA) approach that has received considerable attention from the research community in the past few years [4]- [8]. SCMA provides a spectrally efficient transmission by assigning unique sparse codes to

users who share the wireless medium [9], [10]. The codes' sparsity property enables the use of the iterative message passing algorithm (MPA) at the receiver, to provide a near optimum decoding performance with an implementable decoding complexity [11].

Power-domain NOMA is another variant of NOMA in which users' signals are superposed with different power levels [12]. Power-domain NOMA assisted by the RIS technology has been explored in [13]- [17]. In [13] and [14], the downlink system performance for the RIS-NOMA scheme is improved for single and multiple antenna systems, respectively. The authors in [15] and [16] utilize the RIS to maximize the sum-rate for the downlink millimeter-wave NOMA and uplink NOMA, respectively. The sum coverage range maximization is performed in [17] for a downlink RIS-NOMA system. On the other hand, SCMA and RIS have only been recently explored in [18], [19]. The first investigation in [18] utilizes the RIS technology for reducing the decoding complexity of the conventional uplink SCMA system without optimizing the RIS phase shifts. In contrast, the authors in [19] provide the error rate and sum-rate performance analysis for the uplink RIS-SCMA system. To the best of the authors' knowledge, no published work has investigated the optimization of the RIS phases in detail for RIS-SCMA.

This letter provides two algorithms to optimize the RIS discrete phase shifts of the uplink RIS-SCMA system, for the first time. These algorithms are based on alternate optimization (AO), and are referred to as AO and low-complexity AO (LC-AO). It is worth noting that employing the AO algorithm for the uplink RIS-SCMA requires mathematical manipulation to formulate the system model. The LC-AO algorithm is proposed to provide the same performance as the AO algorithm, but with a significant reduction in the computational complexity. The proposed algorithms considerably improve the received signal-to-noise ratio (SNR) compared to the non-optimized (i.e., blind) scenario by iteratively optimizing the discrete RIS phase shifts. Monte Carlo simulations and complexity analysis are provided to assess the proposed algorithms.

The remainder of this letter is organized as follows: Section II presents the system model of the uplink RIS-SCMA system. The formulation of the optimization problem and the proposed algorithms are introduced in Section III, while their complexity is analyzed in Section IV. Finally, simulation results and conclusions are presented in Sections V and VI, respectively.

II. UPLINK RIS-SCMA SYSTEM MODEL

Fig. 1 illustrates an uplink RIS-SCMA system that consists of U uplink single-antenna users that encode their data using
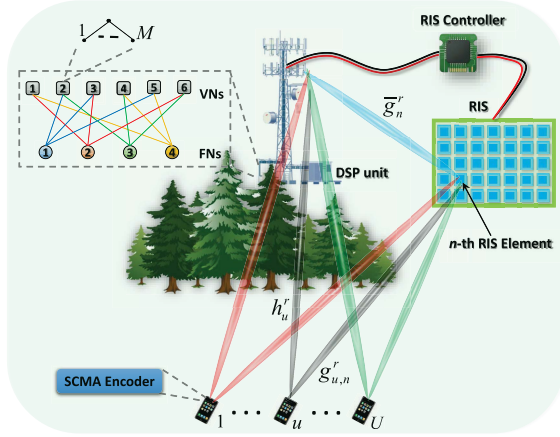
Fig. 1.   Uplink RIS-SCMA system.

unique sparse codebooks, $\mathbf{C}_u \in \mathbb{C}^{R \times M}$, $u = 1, \ldots, U$, where M and R (for code-domain NOMA, $U > R$) are the size of the user's codebook and orthogonal resource elements (OREs), respectively. The user's codebook, $\mathbf{c}_{u,m} \in \mathbb{C}^{R \times 1}$, $m = 1, \ldots, M$, contains d_v non-zero codeword elements. It is worth noting that the sparse codebooks for all users are designed to share the same R OREs in which the number of non-zero shared codeword elements for each ORE, d_f, is fixed. It is assumed that each single-antenna user delivers its data to a single-antenna base station (BS) through a line-of-sight (LoS) path and through an N passive reflecting RIS elements.

The ORE for SCMA can be a frequency-unit or a time-unit depending on the nature of the problem. In this letter, a time-unit ORE is considered for the RIS-SCMA systems. For each ORE, the received signal, y^r, at the receiver-side is given by

$$y^r = \sum_{u \in \Lambda_r} \left(\sum_{n=1}^N \left(g_{u,n}^r e^{-\jmath \phi_n} \bar{g}_n^r + h_u^r \right) \right) c_{u,m}^r + w^r, \quad (1)$$

where h_u^r, $\bar{g}_n^r$ and $g_{u,n}^r$ are the channel coefficients of the u-th user to BS (i.e., the LoS component), n-th RIS element to BS, and u-th user to n-th RIS element, respectively, at the r-th ORE. $c_{u,m}^r$ is the u-th user's codeword at the r-th ORE. The additive white Gaussian noise at the r-th ORE is denoted as $w^r \sim \mathcal{N}(0, \sigma_r^2)$ with zero-mean and variance of σ_r^2; for simplicity, it is assumed that the noise variance for all R OREs is the same. Λ_r denotes the users' indices that are interfering over the r-th ORE. Here, ϕ_n represents the n-th discrete phase shift of the RIS reflecting at the r-th ORE, and its value is taken from a finite set, $\mathcal{L} \in [-\pi, \pi)$, as

$$\phi_n \in \mathcal{L} = \left\{ -\pi, -\pi + \Delta, \ldots, -\pi + (2^b - 1)\Delta \right\} \quad \forall n, \quad (2)$$

where b represents the number of quantization bits for each RIS phase shift, and $\Delta = 2\pi/2^b$ is the step size between two successive discrete values of the RIS phase shifts. At the receiver, the MPA [18] is employed to decode the users' messages by iteratively updating the messages between function nodes (FN) and variable nodes (VN), as illustrated in Fig. 1.

The received SNR at the r-th ORE, Γ^r, is

$$\Gamma^r = \frac{E}{\sigma_r^2} \left| \sum_{u \in \Lambda_r} \left(\sum_{n=1}^N \left(g_{u,n}^r e^{-\jmath \phi_n} \bar{g}_n^r + h_u^r \right) \right) \right|^2, \quad (3)$$

where E is the average transmitted user energy. Here, the optimization of the RIS phase shifts aims to maximize the received SNR at the r-th ORE, as

$$(\text{P1}): \max_{\phi_n} \left| \sum_{u \in \Lambda_r} \left(\sum_{n=1}^N \left(g_{u,n}^r e^{-\jmath \phi_n} \bar{g}_n^r + h_u^r \right) \right) \right|^2 \quad (4)$$

$$\text{s.t. } \phi_n \in \mathcal{L}, \quad \forall n, \ \forall r. \quad (5)$$

The optimization problem in (P1) is non-convex due to the objective function itself and the finite values of the phase shifts. There is no unique method to relax a non-convex problem to obtain an optimal solution efficiently. The optimal solution can be achieved by utilizing an exhaustive search for all combinations of the discrete RIS phase shifts. However, the computational complexity of this approach is practically prohibitive. It is worth noting that optimizing the received SNR can be considered for the RIS-SCMA system due to the shaping gain of the users' sparse codebooks.

III. PROPOSED RIS PHASE SHIFTS OPTIMIZATION

As mentioned before, finding the optimal set of RIS phase shifts requires trying $\sim (2^{bN}R)$ possible combinations, which is extremely costly and infeasible even for a small-scale problem. A sub-optimal solution with acceptable computational complexity can be obtained by utilizing the AO concept. It should be emphasized that the AO algorithm is adopted in [20] for a different wireless communication scheme, here, a reformulation of (P1) is needed to apply the AO algorithm.

A. Proposed AO Algorithm

In the proposed AO algorithm, the solution of (P1) in (4) can be obtained by iteratively optimizing the RIS phase shifts one at a time at each ORE. Consider $\bar{\boldsymbol{g}}_n^r \in \mathbb{C}^{1 \times N} = [\bar{g}_1^r \ldots \bar{g}_n^r \ldots \bar{g}_N^r]$, $\Phi^r \in \mathbb{C}^{N \times N} = \text{diag}([e^{-\jmath\phi_1} \ldots e^{-\jmath\phi_n} \ldots e^{-\jmath\phi_N}])$ with $\text{diag}(\cdot)$ reshaping the corresponding vector to a diagonal square matrix, $\boldsymbol{G}^r \in \mathbb{C}^{N \times d_f} = [\boldsymbol{g}_1^r \ldots \boldsymbol{g}_u^r \ldots \boldsymbol{g}_{d_f}^r]$ with $\boldsymbol{g}_u^r \in \mathbb{C}^{N \times 1} = [g_{u,1}^r \ldots g_{u,n}^r \ldots g_{u,N}^r]^\dagger \ \forall u \in \Lambda_r$, $\boldsymbol{h}^r \in \mathbb{C}^{1 \times d_f} = [h_1^r \ldots h_u^r \ldots h_{d_f}^r] \ \forall u \in \Lambda_r$, and $\boldsymbol{c}^r \in \mathbb{C}^{d_f \times 1} = [c_{1,m}^r \ldots c_{u,m}^r \ldots c_{d_f,m}^r]^\dagger \ \forall u \in \Lambda_r$, with $\dagger$ denoting transpose. Therefore, y^r in (1) and Γ^r in (3) can respectively be written as

$$y^r = \left(\bar{\boldsymbol{g}}_n^r \Phi^r \boldsymbol{G}^r + \boldsymbol{h}^r \right) \boldsymbol{c}^r + w^r, \quad (6)$$

and

$$\Gamma^r = \frac{E}{\sigma_r^2} \left\| \bar{\boldsymbol{g}}_n^r \Phi^r \boldsymbol{G}^r + \boldsymbol{h}^r \right\|^2. \quad (7)$$

The proposed AO algorithm employs an exhaustive search for only one phase shift, while the remaining $N-1$ phase shifts are kept fixed. An iterative procedure is required to improve the performance of the proposed AO algorithm. The optimized phase shift of the n-th RIS element for the r-th ORE, ϕ_n^*, is

$$\phi_n^* = \underset{\phi_{n,t} \in \mathcal{L}}{\arg\max} \ \left\| \bar{\boldsymbol{g}}_n^r \Phi^r(\phi_{n,t}) \boldsymbol{G}^r + \boldsymbol{h}^r \right\|^2, \quad r = 1, \ldots, R, \quad (8)$$

where $\Phi^r(\phi_{n,t}) = \text{diag}([e^{-j\phi_{1,t-1}} \ldots e^{-j\phi_{n,t}} \ldots e^{-j\phi_{N,t-1}}])$ is the phase shifts matrix with only varying $\phi_{n,t}$ at the t-th iteration, while the rest of phase shifts are given by the

Algorithm 1 The Proposed AO Algorithm Pseudo-Code

- **Input:** $\bar{g}_n^r$, G^r, h^r, $\mathcal{L}$, and maximum # of iteration, T;
- **Initiate:** $\phi_{n,0} = 0$ for $n = 1, \ldots, N$;

1: **Set:** $t \leftarrow 1$;
2: **for** $r = 1$ **to** R
3:    **while** $t \leq T$, **do**
4:       **for** $n = 1$ **to** N
5:          **Buffer:** $\zeta_{max} = [\cdot]$;
6:          **for** $l = 1$ **to** 2^b
7:             $\zeta_{max}(1, l) \leftarrow \|\bar{g}_n^r \Phi^r(\phi_{n,t,l}) G^r + h^r\|^2$;
8:          **end for**
9:          **Find:** $i_{max} = \arg \max\{\zeta_{max}\}$;
10:            **Update:** $\phi_{n,t} \leftarrow \mathcal{L}(i_{max})$;
11:       **end for**
12:       **Set:** $t \leftarrow t + 1$;
13:    **end while**
14:    **Set:** $\Phi^r \leftarrow \mathbf{diag}([e^{-j\phi_{1,T}} \ldots e^{-j\phi_{N,T}}])$
15: **end for**
- **Output** Φ^r for $r = 1, \ldots, R$.

previous iteration (i.e., the $(t - 1)$-th iteration). Finally, the algorithm stops after T iterations. Algorithm 1 summarizes the steps of the proposed AO algorithm.

B. Proposed LC-AO Algorithm

As seen from line #7 in Algorithm 1, the AO algorithm calculates some terms that are not a function of $\phi_{n,t}$, in each iteration. Thus, we can achieve the same performance as Algorithm 1 with a significant reduction in computational complexity by eliminating these terms. In this subsection, the target is to find and neglect these unnecessary terms.

To achieve this goal, consider $\bar{g}_n^r \Phi^r G^r = v^r \mathrm{diag}(\bar{g}_n^r) G^r$, where $v^r \in \mathbb{C}^{1 \times N} = [e^{-j\phi_1} \ldots e^{-j\phi_N}]$, and $\Xi^r \in \mathbb{C}^{N \times d_f} = \mathrm{diag}(\bar{g}_n^r) G^r$. Thus, (7) can be written as

$$\Gamma^r = \frac{E}{\sigma_r^2} \|v^r \Xi^r + h^r\|^2$$

$$= \frac{E}{\sigma_r^2} \left(\underbrace{v^r D^r (v^r)^H}_{\text{Term 1}} + \underbrace{2\Re\{v^r \bar{d}^r\}}_{\text{Term 2}} + \|h^r\|^2 \right), \quad (9)$$

where $\Re\{\cdot\}$ returns the real value of a complex number, $D^r \in \mathbb{C}^{N \times N} = \Xi^r (\Xi^r)^H$, and $\bar{d}^r \in \mathbb{C}^{N \times 1} = \Xi^r (h^r)^H$. Thus, the (k, n)-th element of D^r (i.e., $d_{k,n}^r$) and the k-th element of $\bar{d}^r$ (i.e., $\bar{d}_k^r$) are respectively given as

$$d_{k,n}^r = \sum_{i=1}^{d_f} \left(g_{k,i}^r \bar{g}_k^r \right) \left(g_{n,i}^r \bar{g}_n^r \right)^*, \quad (10)$$

and

$$\bar{d}_k^r = \sum_{i=1}^{d_f} \left(g_{k,i}^r \bar{g}_k^r \right) (h_i^r)^*, \quad (11)$$

where $(\cdot)^*$ denotes the conjugate of the complex number.

Now, we need to find the terms in (9) that are not a function of ϕ_n, to be neglected. Term 1 in (9) can be written as

$$v^r D^r (v^r)^H = A_1^r (\phi_n) + A_1^r (\Phi^r \backslash \phi_n), \quad (12)$$

where

$$A_1^r (\phi_n) = 2\Re \left\{ e^{-j\phi_n} \sum_{k \neq n}^N e^{j\phi_k} \left(d_{k,n}^r \right)^* \right\}, \quad (13)$$

and

$$A_1^r (\Phi^r \backslash \phi_n) = \sum_{n=1}^N d_{n,n}^r + 2\Re \left\{ \sum_{i \neq n}^N \sum_{j \neq n}^N e^{j(\phi_i - \phi_j)} \left(d_{i,j}^r \right)^* \right\}. \quad (14)$$

Similarly, Term 2 in (9) can be written as

$$2\Re \left\{ v^r \bar{d}^r \right\} = A_2^r (\phi_n) + A_2^r (\Phi^r \backslash \phi_n), \quad (15)$$

where

$$A_2^r (\phi_n) = 2\Re \left\{ e^{-j\phi_n} \bar{d}_n^r \right\}, \quad (16)$$

and

$$A_2^r (\Phi^r \backslash \phi_n) = 2\Re \left\{ \sum_{i \neq n}^N e^{-j\phi_i} \bar{d}_i^r \right\}. \quad (17)$$

Hence, $A_1^r (\Phi^r \backslash \phi_n)$ in (14), $A_2^r (\Phi^r \backslash \phi_n)$ in (17) and $\|h^r\|^2$ in (9) can be neglected in solving (8) since they are independent of ϕ_n. Consequently, using (13) and (16), the solution of (8) yields

$$\phi_n^* = \arg \max_{\phi_{n,t} \in \mathcal{L}} \Re \left\{ e^{-j\phi_{n,t}} \underbrace{\left(\bar{d}_n^r + \sum_{k \neq n}^N e^{j\phi_{k,t-1}} (d_{k,n}^r)^* \right)}_{\text{Term 3}} \right\}, \quad (18)$$

where $d_{k,n}^r$ and $\bar{d}_n^r$ are given by (10) and (11), respectively. Iterations are also required to improve the performance of (18). It is worth noting that the LC-AO algorithm calculates Term 3 in (18) only once for all 2^b possible combinations of ϕ_n. Algorithm 2 summarizes the proposed LC-AO algorithm.

IV. COMPLEXITY ANALYSIS

The computational complexity of the proposed AO and LC-AO algorithms is derived in terms of the real additions and real multiplications. For the AO algorithm, the matrix and vector operation inside the norm in (8) requires $2N(2d_f + 1)$ and $4N(d_f + 1)$ real additions and multiplications, respectively, for each possible value of ϕ_n. Furthermore, the second norm performs $(2d_f - 1)$ and $2d_f$ real additions and multiplications, respectively. Thus, the total number of real additions, $\mathrm{RA_{AO}}$, and multiplications, $\mathrm{RM_{AO}}$, required to perform the AO algorithm is respectively given as

$$\mathrm{RA_{AO}} = RN2^b \left(2N \left(2d_f + 1 \right) + 2d_f - 1 \right), \quad (19)$$
$$\mathrm{RM_{AO}} = RN2^b \left(4N \left(d_f + 1 \right) + 2d_f \right). \quad (20)$$

In the proposed LC-AO algorithm, (10) and (11) require $(8d_f - 2)$ and $(6d_f - 2)$ real additions, as well as $12d_f$ and $8d_f$ real multiplications, respectively. Thus, Term 3 in (18) requires $N(8d_f + 1) - 2(d_f + 1)$ and $4N(3d_f + 1) - 4(d_f + 1)$ real additions and multiplications, respectively. It is worth noting that the LC-AO algorithm calculates Term 3 only once for all 2^b possibilities of ϕ_n. Therefore, the total number of real

Algorithm 2 The Proposed LC-AO Algorithm Pseudo-Code

- **Input:** $\bar{g}_n^r$, $\boldsymbol{G}^r$, $\boldsymbol{h}^r$, $\mathcal{L}$, and maximum # of iteration, T;
- **Initiate:** $\phi_{n,0} = 0$ for $n = 1, \ldots, N$;

1: **Set:** $t \leftarrow 1$;
2: **for** $r = 1$ **to** R
3:    **while** $t \leq T$, **do**
4:       **for** $n = 1$ **to** N
5:          **Buffer:** $\zeta_{max} = [\cdot]$, and $\psi_n^r = [\cdot]$;
6:          **for** $k = 1$ **to** N
7:             **if** $k \neq n$, **do**
8:                $d_{k,n}^r = \sum_{i=1}^{d_f} \left(g_{k,i}^r \bar{g}_k^r \right) \left(g_{n,i}^r \bar{g}_n^r \right)^*$;
9:                **Set:** $\psi_n^r \leftarrow \psi_n^r + e^{j\phi_{k,t-1}} (d_{k,n}^r)^*$;
10:            **end if**
11:         **end for**
12:         **Compute:** $\bar{d}_n^r = \sum_{i=1}^{d_f} \left(g_{n,i}^r \bar{g}_n^r \right) (h_i^r)^*$;
13:         **Compute: Term 3** $= \bar{d}_n^r + \psi_n^r$;
14:         **for** $l = 1$ **to** 2^b
15:            $\zeta_{max}(1,l) \leftarrow \Re \left\{ e^{-j\phi_{n,t,l}} \times \textbf{Term 3} \right\}$;
16:         **end for**
17:         **Find:** $i_{max} = \arg\max\{\zeta_{max}\}$;
18:            **Update:** $\phi_{n,t} \leftarrow \mathcal{L}(i_{max})$;
19:      **end for**
20:      **Set:** $t \leftarrow t + 1$;
21:   **end while**
22:   **Set:** $\Phi^r \leftarrow \textbf{diag}([e^{-j\phi_{1,T}} \ldots e^{-j\phi_{N,T}}])$
23: **end for**

- **Output** Φ^r for $r = 1, \ldots, R$.

additions, $\text{RA}_{\text{LC-AO}}$, and multiplications, $\text{RM}_{\text{LC-AO}}$, required to perform the LC-AO algorithm are respectively given as

$$\text{RA}_{\text{LC-AO}} = RN \left(2^{b+1} + N \left(8d_f + 1 \right) - 2 \left(d_f + 1 \right) \right), \quad (21)$$

$$\text{RM}_{\text{LC-AO}} = RN \left(2^{b+2} + 4N \left(3d_f + 1 \right) - 4 \left(d_f + 1 \right) \right). \quad (22)$$

V. SIMULATION RESULTS

In this section, Monte Carlo simulations are used to evaluate the proposed AO and LC-AO algorithms for uplink RIS-SCMA. The codebooks for all users are set based on the approach in [10]. The parameters employed in simulations are $U = 6$, $R = 4$, $d_f = 3$, $b = 3$, $T = 3$, and $M = 2$. As depicted in Fig. 2, the simulation setup is as follows: $d = 40$ m, $d_p = 1.5$ m, $d_1 = \sqrt{d_p^2 + d_o^2}$ m, and $d_2 = \sqrt{d_p^2 + (d - d_o)^2}$ m. The overall system path loss is $(\lambda^4 d_1^{-2} d_2^{-2})/(256\pi^2)$ [21], where λ denotes the signal wavelength for the 2.4 GHz operating frequency. All channels are Rician fading with a factor of 1. The average received SNR of the RIS-SCMA system for all R OREs, Γ, in dB is used to assess the behavior of the proposed optimization algorithms. The blind scenario mentioned in the simulation results refers to the case where the RIS reflects the incident signals without performing any optimization on the phase shifts (i.e., $\phi_n = 0$, $\forall n$ and $\forall r$). This scenario is included only to show the gain obtained from comparing the optimized scenario with the non-optimized one.

Fig. 3 considers the deployment of the RIS for the uplink RIS-SCMA system. This investigation involves varying d_0 (from the BS towards the users) for different values of the RIS elements, i.e., $N = 16$, 32 and 64. It is shown that the
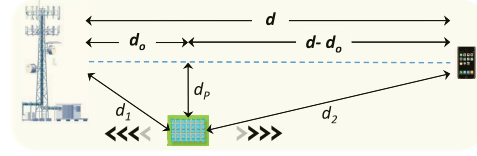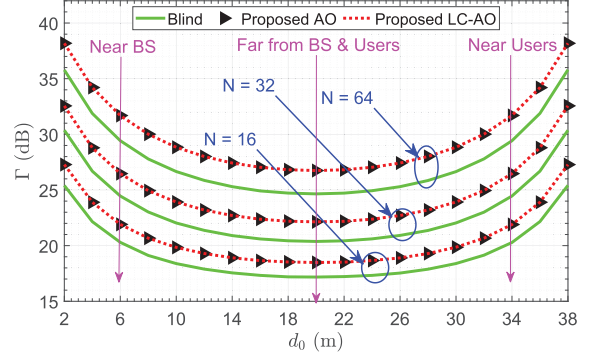

Fig. 2.   Simulation setup.

Fig. 3.   Deployment investigation of the RIS for the uplink RIS-SCMA system.
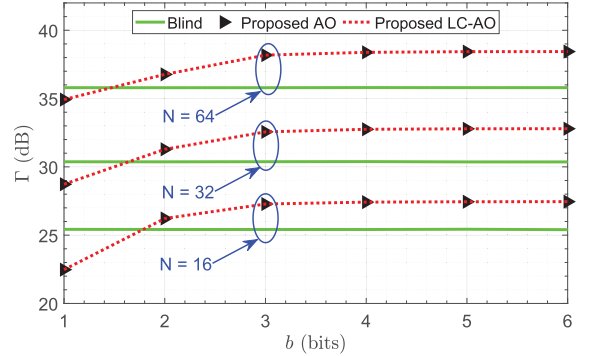

Fig. 4.   Effect of the quantization bits for each RIS phase shift.

maximum average received SNR occurs when the RIS is either near the BS or near the users. In this letter, we consider that the RIS is placed near the BS with $d_0 = 2$ m. Further, results also show that the proposed AO and LC-AO algorithms provide the same received SNR and outperform the blind scenario.

Fig. 4 depicts the average received SNR at $d_0 = 2$ m versus different RIS phase shift values for different values of N. The proposed AO and LC-AO algorithms provide the same received SNR, and outperform the blind scenario in terms of the received SNR when $b \geq 2$. As seen from Fig. 4, the improvement of the received SNR of the proposed algorithms saturates when $b \geq 3$. Furthermore, the computational complexity of the proposed algorithms increases as b increases, according to Section IV. Thus, $b = 3$ is selected. It should be pointed out that for $b = 1$, only two phase shift values are available for each RIS element (i.e., $\mathcal{L} = \{-\pi, 0\}$ in (5)), which is not enough to improve the performance over the blind scenario.

Fig. 5a shows that only three iterations (i.e., $T = 3$) are enough for the proposed algorithms to converge. Therefore, at $d_o = 2$ m, $b = 3$ and $T = 3$, the average received SNR of the proposed AO and LC-AO algorithms is the same and increases as N increases, as shown in Fig. 5b. It is also seen that the proposed algorithms provide a significant improvement in the received SNR compared to the blind and
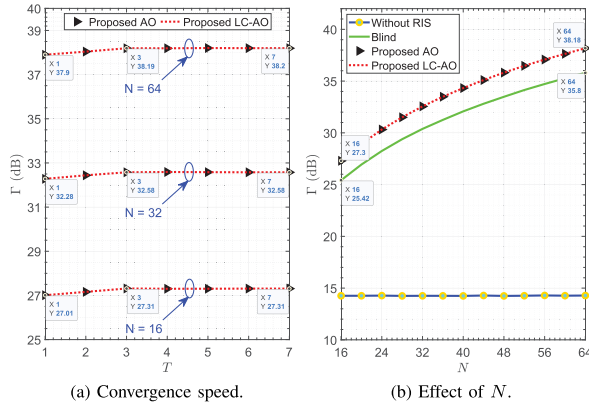
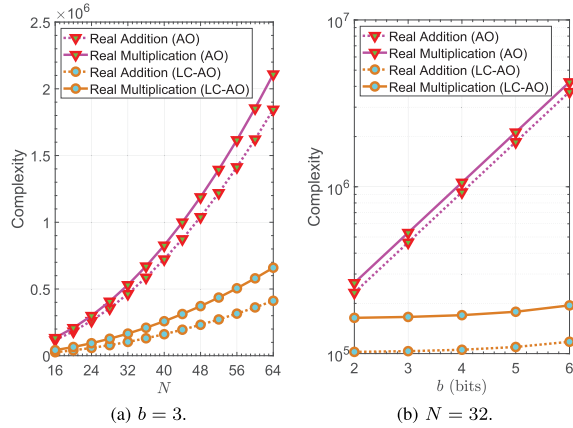Fig. 5. Convergence speed and effect of N on the proposed algorithms for the uplink RIS-SCMA system.

Fig. 6. Complexity comparison of the proposed algorithms.

without RIS scenarios; e.g., the proposed algorithms provide 1.88 dB and 2.38 dB improvement in the received SNR at $N = 16$ and 64, respectively, compared to the blind scenario.

As seen from Fig. 6 and Section IV, the proposed LC-AO algorithm significant reduces the computational complexity in terms of the number of real additions and multiplications. The complexity of the AO algorithm significantly increases as N increases, while that of the LC-AO algorithm increases less with N, as illustrated in Fig. 6a. Furthermore, unlike the AO algorithm, the complexity of the LC-AO algorithm slightly increases as b increases, as shown in Fig. 6b.

Finally, the proposed algorithms provide up to 2.4 dB improvement in the received SNR compared with the blind scenario. Besides, the complexity of the proposed LC-AO algorithm is significantly lower when compared with that of the AO algorithm for the same received SNR.

VI. CONCLUSION

For the first time, this letter has proposed an alternate optimization algorithm to optimize the uplink RIS-SCMA discrete phase shifts, namely, the AO algorithm. Furthermore, a novel variant of the AO algorithm has been introduced, referred to as the LC-AO algorithm; this has achieved the same received SNR as the AO algorithm, but with a significant reduction in computational complexity. The deployment and optimal number of discrete phase shifts for RIS have been investigated. The simulation results have shown that placing the RIS near the BS or users is beneficial, while the 3-bit quantization for RIS phase shifts is enough to improve the received SNR

with an acceptable complexity. The proposed algorithms have significantly improved the received SNR compared to the blind scenario, and this improvement increases with the number of RIS elements. The system model can be extended to include multiple antennas for the BS and users in the future work.

REFERENCES

[1] E. Basar, M. Di Renzo, J. De Rosny, M. Debbah, M. Alouini, and R. Zhang, "Wireless communications through reconfigurable intelligent surfaces," *IEEE Access*, vol. 7, pp. 116753–116773, 2019.

[2] M. A. El Mossallamy, H. Zhang, L. Song, K. G. Seddik, Z. Han, and G. Y. Li, "Reconfigurable intelligent surfaces for wireless communications: Principles, challenges, and opportunities," *IEEE Trans. Cogn. Commun. Netw.*, vol. 6, no. 3, pp. 990–1002, Sep. 2020.

[3] E. Basar, "Transmission through large intelligent surfaces: A new frontier in wireless communications" in *Proc. Eur. Conf. Netw. Commun. (EuCNC)*, Jun. 2019, pp. 112–117.

[4] M. Rebhi, K. Hassan, K. Raoof, and P. Chargé, "Sparse code multiple access: Potentials and challenges," *IEEE Open J. Commun. Soc.*, vol. 2, pp. 1205–1238, 2021.

[5] S. M. R. Islam, N. Avazov, O. A. Dobre, and K.-S. Kwak, "Power-domain non-orthogonal multiple access (NOMA) in 5G systems: Potentials and challenges," *IEEE Commun. Surveys Tuts.*, vol. 19, no. 2, pp. 721–742, 2nd Quart., 2016.

[6] Z. Ding, X. Lei, G. K. Karagiannidis, R. Schober, J. Yuan, and V. Bhargava, "A survey on non-orthogonal multiple access for 5G networks: Research challenges and future trends," *IEEE J. Sel. Areas Commun.*, vol. 35, no. 10, pp. 2181–2195, Oct. 2017.

[7] I. Al-Nahhal, O. A. Dobre, E. Basar, and S. Ikki, "Low-cost uplink sparse code multiple access for spatial modulation," *IEEE Trans. Veh. Technol.*, vol. 68, no. 9, pp. 9313–9317, Sep. 2019.

[8] I. Al-Nahhal, O. A. Dobre, and S. Ikki, "On the complexity reduction of uplink sparse code multiple access for spatial modulation," *IEEE Trans. Commun.*, vol. 68, no. 11, pp. 6962–6974, Nov. 2020.

[9] H. Nikopour and H. Baligh, "Sparse code multiple access," in *Proc. IEEE Int. Symp. Pers. Indoor Mobile Radio Commun. (PIMRC)*, Sep. 2013, pp. 332–336.

[10] M. Taherzadeh, H. Nikopour, A. Bayesteh, and H. Baligh, "SCMA codebook design," in *Proc. IEEE 80th Veh. Technol. Conf. (VTC-Fall)*, Sep. 2014, pp. 1–5.

[11] H. Mu, Z. Ma, M. Alhaji, P. Fan, and D. Chen, "A fixed low complexity message pass algorithm detector for up-link SCMA system," *IEEE Wireless Commun. Lett.*, vol. 4, no. 6, pp. 585–588, Dec. 2015.

[12] G. Gui, H. Sari, and E. Biglieri, "A new definition of fairness for non-orthogonal multiple access," *IEEE Commun. Lett.*, vol. 23, no. 7, pp. 1267–1271, May 2019.

[13] T. Hou, Y. Liu, Z. Song, X. Sun, Y. Chen, and L. Hanzo, "Reconfigurable intelligent surface aided NOMA networks," *IEEE J. Sel. Areas Commun.*, vol. 38, no. 11, pp. 2575–2588, Nov. 2020.

[14] T. Hou, Y. Liu, Z. Song, X. Sun, and Y. Chen, "MIMO-NOMA networks relying on reconfigurable intelligent surface: A signal cancellation-based design," *IEEE Trans. Commun.*, vol. 68, no. 11, pp. 6932–6944, Nov. 2020.

[15] J. Zuo, Y. Liu, E. Basar, and O. A. Dobre, "Intelligent reflecting surface enhanced millimeter-wave NOMA systems," *IEEE Commun. Lett.*, vol. 24, no. 11, pp. 2632–2636, Nov. 2020.

[16] M. Zeng, X. Li, G. Li, W. Hao, and O. A. Dobre, "Sum rate maximization for IRS-assisted uplink NOMA," *IEEE Commun. Lett*, vol. 25, no. 1, pp. 234–238, Jan. 2021.

[17] C. Wu, Y. Liu, X. Mu, X. Gu, and O. A. Dobre, "Coverage characterization of STAR-RIS networks: NOMA and OMA," *IEEE Commun. Lett.*, vol. 25, no. 9, pp. 3036–3040, Sep. 2021, doi: 10.1109/LCOMM.2021.3091807.

[18] I. Al-Nahhal, O. A. Dobre, and E. Basar, "Reconfigurable intelligent surface-assisted uplink sparse code multiple access," *IEEE Commun. Lett.*, vol. 25, no. 6, pp. 2058–2062, Jun. 2021.

[19] S. Sharma, K. Deka, Y. Hong, and D. Dixit, "Intelligent reflecting surface-assisted uplink SCMA system," *IEEE Commun. Lett.*, vol. 25, no. 8, pp. 2728–2732, Aug. 2021, doi: 10.1109/LCOMM.2021.3081569.

[20] Q. Wu and R. Zhang, "Intelligent reflecting surface enhanced wireless network via joint active and passive beamforming," *IEEE Trans. Wireless Commun.*, vol. 18, no. 11, pp. 5394–5409, Nov. 2019.

[21] S. W. Ellingson, "Path loss in reconfigurable intelligent surface-enabled channels," 2019, *arXiv:1912.06759*. [Online]. Available: http://arxiv.org/abs/1912.06759